

Spin State Change in Organometallic Reactions. Experimental and MP2 Theoretical Studies of the Thermodynamics and Kinetics of the CO and N₂ Addition to Spin Triplet Cp*MoCl(PMe₃)₂

D. Webster Keogh and Rinaldo Poli^{*,†}

Contribution from the Department of Chemistry and Biochemistry, University of Maryland, College Park, Maryland 20742

Received March 11, 1996. Revised Manuscript Received October 21, 1996[⊗]

Abstract: The first comparative kinetic study of the addition of the isolobal and isosteric CO and N₂ ligands to a spin triplet organometallic compound, i.e. Cp*MoCl(PMe₃)₂, is reported. A fast and quantitative addition process occurred when interacting Cp*MoCl(PMe₃)₂ with CO, which is followed by a subsequent slower process involving PMe₃ replacement and formation of Cp*MoCl(CO)₂(PMe₃). The N₂ addition, on the other hand, is much slower and proceeds incompletely to an equilibrium position. The temperature dependence of this equilibrium gives the parameters for the reaction $\Delta H = -22.8 \pm 2.1$ kcal/mol and $\Delta S = -67 \pm 7$ cal·mol⁻¹·K⁻¹. The activation parameters for the CO addition are $\Delta H^\ddagger = 5.0 \pm 0.3$ kcal/mol and $\Delta S^\ddagger = -35 \pm 4$ cal·mol⁻¹·K⁻¹, while the activation parameters for the N₂ addition are $\Delta H^\ddagger = 14.0 \pm 1.0$ kcal/mol and $\Delta S^\ddagger = -20 \pm 3$ kcal/mol. Extrapolation of the rates to 25 °C indicates a difference of more than three orders of magnitude: $k_{\text{CO}} = 29 \pm 3$ M⁻¹ s⁻¹ and $k_{\text{N}_2} = 0.014 \pm 0.001$ M⁻¹ s⁻¹. Theoretical calculations with full geometry optimization at the MP2 level have been carried out on the model systems CpMoCl(PH₃)₂ + L (L = CO or N₂), the calculated energetics of the system being in agreement with experiment. The 16-electron CpMoCl(PH₃)₂ molecule is found to be more stable in the spin triplet state, the excited ¹A' state being 10.9 kcal/mol higher in energy. The Mo–L bond formation is calculated to be exothermic by 27.9 kcal/mol for L = N₂ and by 60.0 kcal/mol for L = CO. Calculations along the L addition coordinate show an initial ligand rearrangement related barrier for both the spin singlet and the spin triplet surfaces. After overcoming this barrier, the spin singlet curve descends in energy earlier for the CO vs the N₂ addition as expected from greater diffuseness of the CO donor and acceptor orbitals. As the N₂ ligand continues to approach the metal, the ³A'' surface becomes increasingly repulsive whereas the addition of CO leads to an attractive interaction and a bound triplet state.

Introduction

The question of whether a change of spin state can slow organometallic reactions has long been debated, and no general agreement seems to have been reached.^{1–4} A spin barrier was proposed to rationalize the slower reaction of CO with spin triplet Fe(CO)₄ ($k = 3.1 \pm 0.7 \times 10^7$ M⁻¹ s⁻¹) with respect to the spin singlet Ru(CO)₄ and Os(CO)₄ ($1.7 \pm 0.5 \times 10^{10}$ and $3.3 \pm 0.4 \times 10^{10}$ M⁻¹ s⁻¹, respectively) and the slower reaction of Fe(CO)₅ with spin triplet Fe(CO)₄ with respect to spin singlet [Fe(CO)₄][†] (e.g. $3.1 \pm 0.9 \times 10^8$ M⁻¹ s⁻¹ vs $k = 1.1 \pm 0.2 \times 10^{11}$ M⁻¹ s⁻¹).^{5,6} The CO additions to Cp₂V ($S = 3/2$), Cp-(pd')V (pd' = η⁵-2,4-dimethylpentadienyl, $S = 1/2$), and (pd)₂V (pd = η⁵-pentadienyl, $S = 1/2$) proceed at comparable rates ($k = 91 \pm 5$, 34 ± 5 , and 42 ± 5 M⁻¹ s⁻¹, respectively), in spite of the spin state difference of the starting materials.⁷ Finally, the addition of CpCo(CO)₂ to spin triplet CpCo(CO) to afford

the diamagnetic Cp₂Co₂(CO)₃ compound proceeds at the near-diffusion-limited rate of $8.8 \pm 0.2 \times 10^9$ M⁻¹ s⁻¹,⁸ and the CO addition to spin triplet Tp'Co(CO) (Tp' = hydrotris(3-isopropyl-5-methylpyrazolyl)borate) at 224 K to afford diamagnetic Tp'Co(CO)₂ is also close to the diffusion limit, $k = 3 \pm 1 \times 10^9$ M⁻¹ s⁻¹.⁴ However, other reactions that cause a spin flip, notably oxidative additions of H₂ and C–H bonds, are found to be much slower in cases where CO adds extremely rapidly.¹ Although the orbital requirements for the CO addition and H₂ oxidative addition are the same (donation from the C lone pair or H–H σ bond to an empty metal orbital, back-donation from filled metal orbitals to the two C–O π* or the single H–H σ* empty orbital(s)), the two reactions lead to different geometries and states of hybridization in the product and possibly also in the transition state. A recent theoretical paper by Siegbahn attributes the experimentally established⁸ lack of C–H oxidative addition to $S = 1$ CpCo(CO) to the spin change barrier, which is absent in the corresponding facile process of CpRh(CO).⁹

We have recently reported that the spin triplet, 16-electron complex Cp*MoCl(PMe₃)₂ reacts with both CO and N₂ to form the corresponding diamagnetic adducts.¹⁰ We have therefore proceeded to investigate, for the first time, the comparative rates of CO and N₂ addition to the same unsaturated spin triplet system, the results of which allow us to make new considerations on the importance of a spin state change in the rates of ligand

[†] Current address: Laboratoire de Synthèse et d'Électrosynthèse Organométallique, Faculté des Sciences "Gabriel", 6, Boulevard Gabriel, 21100 Dijon, France.

[⊗] Abstract published in *Advance ACS Abstracts*, March 1, 1997.

(1) Brintzinger, H. H.; Lohr, L. L., Jr.; Wong, K. L. T. *J. Am. Chem. Soc.* **1975**, *97*, 5146–5155.

(2) Janowicz, A. H.; Bryndza, H. E.; Bergman, R. G. *J. Am. Chem. Soc.* **1981**, *103*, 1516–1518.

(3) Schrock, R. R.; Shih, K.-Y.; Dobbs, D. A.; Davis, W. M. *J. Am. Chem. Soc.* **1995**, *117*, 6609–6610.

(4) Detrich, J. L.; Reinaud, O. M.; Rheingold, A. L.; Theopold, K. H. *J. Am. Chem. Soc.* **1995**, *117*, 11745–11748.

(5) Bogdan, P. L.; Weitz, E. *J. Am. Chem. Soc.* **1989**, *111*, 3163–3167.

(6) Ryther, R. J.; Weitz, E. *J. Phys. Chem.* **1991**, *95*, 9841–9852.

(7) Kowaleski, R. M.; Basolo, F.; Trogler, W. C.; Gedridge, R. W.; Newbound, T. D.; Ernst, R. D. *J. Am. Chem. Soc.* **1987**, *109*, 4860–4869.

(8) Bengali, A. A.; Bergman, R. G.; Moore, C. B. *J. Am. Chem. Soc.* **1995**, *117*, 3879–3880.

(9) Siegbahn, P. E. M. *J. Am. Chem. Soc.* **1996**, *118*, 1487–1496.

(10) Abugideiri, F.; Keogh, D. W.; Poli, R. *J. Chem. Soc., Chem. Commun.* **1994**, 2317–2318.

addition reactions. We also report theoretical calculations aimed at understanding the difference in activation energy for the CO and N₂ additions and at assessing the importance of electron pairing for the thermodynamic stabilization of the open-shell CpMoCl(PH₃)₂ system.

Experimental Section

General Procedures. All operations were carried out under an atmosphere of argon with standard Schlenk-line techniques unless noted otherwise. Solvents were purified by conventional methods and distilled under argon prior to use. FT-IR spectra were recorded on a Perkin-Elmer 1800 spectrophotometer with KBr disks. NMR spectra were obtained with Bruker WP200 and AF200 spectrometers: peak positions are reported with positive shifts downfield of TMS as calculated from residual solvent peaks (¹H) or downfield of external 85% H₃PO₄ (³¹P). For each ³¹P-NMR spectrum, a sealed capillary containing H₃PO₄ was immersed in the same NMR solvent used for the measurement and this was used as the reference. Cp*MoCl(PMe₃)₂ was prepared as previously described.^{10,11} CO and N₂ were purchased from Air Products and used without further purification.

Gas-Volumetric Measurements. The apparatus used for the gas uptake kinetics and equilibrium studies was a thermostated gas buret similar to that previously described.¹² The only modification consists of the use of a Hg filled, sealed, stainless steel cylinder with a screw controlled piston to adjust the level of Hg in the buret, in place of the open ended glass bulb previously described. The amount of gas consumed was calculated from measured volume change, temperature, and pressure (barometric pressure corrected for the solvent vapor pressure) by using the ideal gas law. The concentration of the gases in solution was calculated using the published equations for the mole fraction of the gas as a function of temperature.¹³

Kinetic Studies of CO and N₂ Addition to Cp*MoCl(PMe₃)₂. For each kinetic experiment an aliquot (1 mL) of a THF solution of Cp*MoCl(PMe₃)₂ was placed into a small thin-walled glass bulb. The neck of the bulb was plugged with glass wool and the reaction bulb flame sealed. The sealed glass bulb was then placed into the reaction vessel, consisting of a 50-mL Erlenmeyer flask equipped with a stopcock sidearm and a 24/40 ground glass joint. THF (10 mL) was then added to the reaction vessel along with a medium sized stirring bar. The atmosphere of the reaction vessel was evacuated and then attached to the gas buret. The gas buret and the reaction vessel were then charged with the appropriate gas and thermostated to the desired temperature. After thermal equilibration, stirring was begun, causing the reactant bulb to break and the reaction to begin. After adjusting for the initial pressure change caused by the breaking bulb, the reaction was monitored by measuring the volume of gas absorbed. The monitoring continued until an equilibrium was reached. For the N₂ reaction, the initial concentration of Cp*MoCl(PMe₃)₂ was determined by introducing a known quantity of ferrocene into the reaction vessel, replacing the atmosphere with H₂, allowing the reaction to proceed for 30 min, and then analyzing the products by ¹H-NMR. It has been previously reported that the 16-electron Cp*MoCl(PMe₃)₂ quantitatively reacts with H₂ to produce the dihydride complex Cp*MoCl(H)₂(PMe₃)₂.¹⁰ Integration of the resonances corresponding to Cp*MoCl(H)₂(PMe₃)₂ and Cp*MoCl(N₂)(PMe₃)₂ against the ferrocene afforded the initial moles of Cp*MoCl(PMe₃)₂. A direct integration of the resonances of Cp*MoCl(PMe₃)₂ and Cp*MoCl(N₂)(PMe₃)₂ is unacceptable because of the inaccuracy in the integration of the resonances for the paramagnetic species. For the CO reaction, the integration of the resonances of the Cp*MoCl(CO)(PMe₃)₂ and Cp*MoCl(CO)₂(PMe₃) products (see Results) against a ferrocene standard gave the initial concentration of Cp*MoCl(PMe₃)₂.

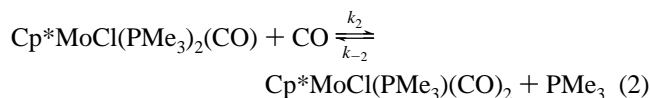
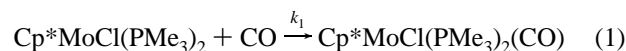
Theoretical Calculations. MP2 geometry optimizations were carried out with the Gaussian 94 package. The LANL2DZ basis set without polarization basis functions includes both Dunning and Hay's

D95 sets for H and C and relativistic ECP sets of Hay and Wadt for the heavy atoms.^{14–16} Electrons outside of the core were all those of H, C, O, and N atoms, the 4s, 4p, 4d, and 5s electrons in the Mo and the 3s and 3p electrons in Cl and P atoms. The mean value of the spin of the first order electron wave function, which is not an exact eigenstate of S² for unrestricted open-shell systems, was considered to identify unambiguously the spin state. The input coordinates were adapted from the known structure of Cp*MoCl(dppe)¹¹ for both ³A' and ¹A' CpMoCl(PH₃)₂ and from the structure of Cp*MoCl(PMe₂Ph)₂(CO)¹¹ for CpMoCl(PH₃)₂L (L = CO or N₂), and were idealized in each case to C_s symmetry. The calculations along the reaction coordinates for CO and N₂ addition to ¹A' and ³A'' CpMoCl(PH₃)₂ were carried out at various Mo–C or Mo–N distances by holding such distances fixed and optimizing the rest of the geometry in C_s symmetry.

Results

Kinetic Studies. The synthesis and characterization of coordinatively unsaturated Mo(II), 16-electron complexes of the type RingMoClL₂ (Ring = Cp, L = PMe₂Ph; Ring = Cp*, L₂ = (PMe₃)₂, (PMe₂Ph)₂, and dppe) has been recently described.^{10,11} These complexes are paramagnetic, with a S = 1 ground state. One of the properties of these unsaturated complexes is their propensity to add 2-electron donor ligands, i.e. CO, N₂, and H₂, to afford stable diamagnetic 18-electron complexes. The dinitrogen adduct Cp*MoCl(N₂)(PMe₃)₂ had previously been obtained by direct reduction of Cp*MoCl₄ in the presence of PMe₃ under N₂.¹⁷ The focus of this paper is the kinetic analysis of the addition of isoelectronic and isosteric pairs of ligands CO and N₂ to Cp*MoCl(PMe₃)₂. In both cases, the additions of these ligands are slightly but not insurmountably complicated by the presence of an equilibrium (vide infra).

The initial addition of CO to Cp*MoCl(PMe₃)₂ is rapid and quantitative (eq 1).^{10,11} After the initial addition, a second and much slower process occurs, i.e. a substitution of a PMe₃ ligand for a second CO (eq 2). This result is indicated by the presence of three ν_{CO} in the IR spectrum of the final mixture at 1782, 1851, and 1946 cm⁻¹, the former of which is attributed to Cp*MoCl(PMe₃)₂(CO),¹⁰ while the latter two are assigned to the symmetric and antisymmetric stretches of the dicarbonyl complex. The blue shift of the carbonyl stretching frequencies is consistent with the removal of electron density from the metal center by substituting a good σ-donor phosphine with a π-acidic carbonyl ligand. A similar trend has been observed for the hydride system, Cp*MoH(CO)_x(PMe₃)_{3-x} (x = 1 or 2).¹⁸ In this case the reported frequencies were 1800, 1860, and 1960 cm⁻¹, with the former value being assigned to Cp*MoH(CO)-(PMe₃)₂ and the latter two to the dicarbonyl species. As a result, the overall reaction results in an equilibrium mixture of Cp*MoCl(PMe₃)₂(CO) and Cp*MoCl(PMe₃)₂(CO)₂. Since the kinetic experiments were run under constant pressure, the [CO] in solution was constant leading to pseudo-first-order conditions.



The k₁ values were obtained from a fit of the gas volume data in the different runs, which were performed over the

(14) Hay, P. J.; Wadt, W. R. *J. Chem. Phys.* **1985**, *82*, 299–310.

(15) Wadt, W. R.; Hay, P. J. *J. Chem. Phys.* **1985**, *82*, 284–298.

(16) Hay, P. J.; Wadt, W. R. *J. Chem. Phys.* **1985**, *82*, 270–283.

(17) Baker, R. T.; Calabrese, J. C.; Harlow, R. L.; Williams, I. D. *Organometallics* **1993**, *12*, 830–841.

(18) Tudoret, M.-J.; Robo, M.-L.; Lapinte, C. *Organometallics* **1992**, *11*, 1419–1422.

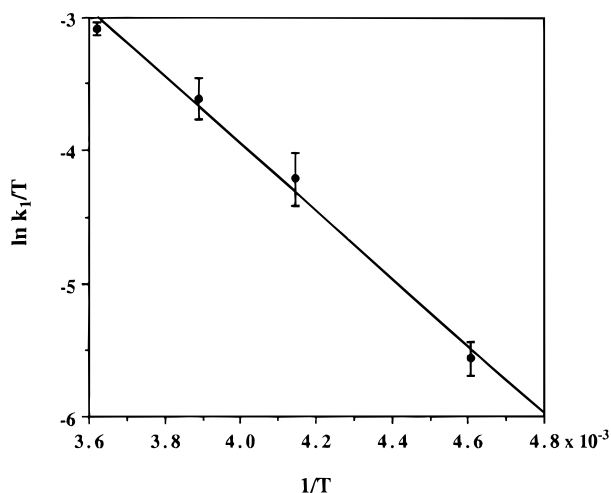
(11) Abugideiri, F.; Fettingner, J. C.; Keogh, D. W.; Poli, R. *Organometallics* **1996**, *15*, 4407–4416.

(12) Calderazzo, F.; Cotton, F. A. *Inorg. Chem.* **1962**, *1*, 30–36.

(13) Fogg, P. G. T.; Gerrard, W. *Solubility of gases in liquids: a critical evaluation of gas/liquid systems in theory and practice*; J. Wiley: New York, 1991; p 332.

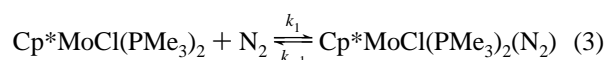
Table 1. Results of the Kinetic Analysis for the Cp*MoCl(PMe₃)₂/CO System

<i>T</i> , °C	10 ³ [Cp*MoCl(PMe ₃) ₂] ₀ , M	10 ³ [CO], M	<i>k</i> ₁ , M ⁻¹ s ⁻¹
-56	2.18 ± 0.07	9.10 ± 0.02	0.840 ± 0.053
-32	3.63 ± 0.12	8.77 ± 0.02	3.54 ± 0.37
-16	2.49 ± 0.08	8.63 ± 0.02	6.94 ± 0.55
3	9.01 ± 0.29	8.45 ± 0.02	12.6 ± 0.3

**Figure 1.** Plot of $\ln(k_1/T)$ versus $1/T$ for the CO addition to Cp*MoCl(PMe₃)₂.

temperature range -56 to +3 °C, to the standard kinetic model of eqs 1 and 2 as the sum of two exponentials.¹⁹ The results are given in Table 1. An Eyring analysis (Figure 1) allowed the determination of the activation parameters, which for eq 1 were $\Delta H^\ddagger = 5.0 \pm 0.3$ kcal and $\Delta S^\ddagger = -35 \pm 4$ cal·mol⁻¹·K⁻¹. The large negative entropy of activation is consistent with the expected ordering in the transition state.

The analysis of the N₂ addition reaction is less complicated, because the formation of the dinitrogen adduct is not followed by further substitution chemistry. On the other hand, the formation of the N₂ adduct is itself an equilibrium process (eq 3). As a result, the rate law is two-termed, accounting for the forward and reverse reactions as shown in eq 4.



$$\text{rate} = k_1[\text{Cp}^*\text{MoCl}(\text{PMe}_3)_2][\text{N}_2] - k_{-1}[\text{Cp}^*\text{MoCl}(\text{PMe}_3)_2(\text{N}_2)] \quad (4)$$

The N₂ kinetic runs were performed at constant N₂ pressure as for the above described CO addition reaction, leading to pseudo-first-order conditions. The analysis of the data followed eqs 5 and 6.

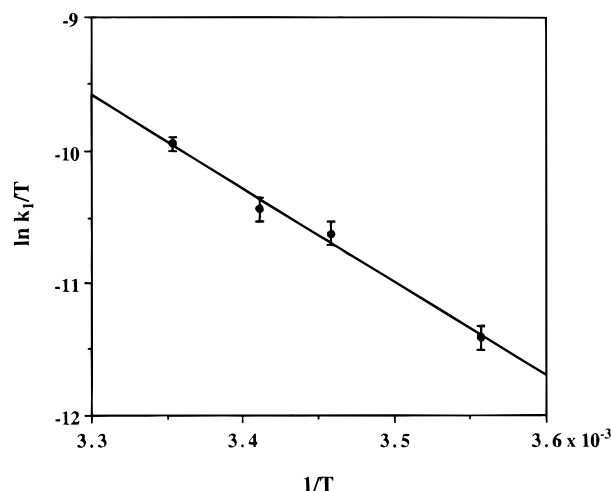
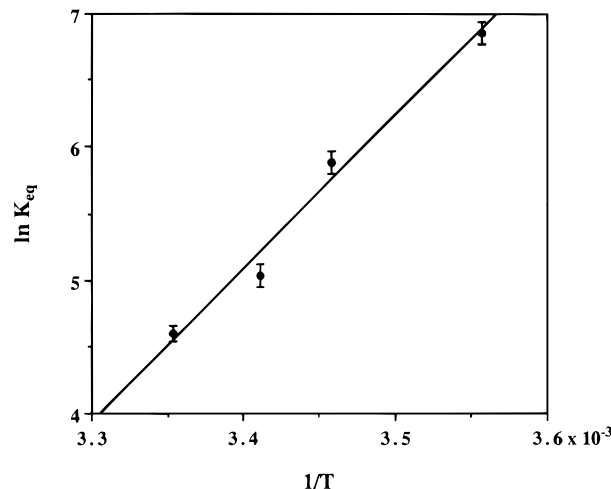
$$k_{\text{obs}} = k_1[\text{N}_2] + \frac{k_1}{K_{\text{eq}}} \quad (5)$$

$$K_{\text{eq}} = \frac{[\text{Cp}^*\text{MoCl}(\text{PMe}_3)_2(\text{N}_2)]}{[\text{Cp}^*\text{MoCl}(\text{PMe}_3)_2][\text{N}_2]} \quad (6)$$

The results of the kinetic experiments for the addition of N₂ to Cp*MoCl(PMe₃)₂ over the temperature range 8 to 25 °C are given in Table 2. It is immediately evident from comparing Tables 1 and 2 that the N₂ addition is much slower than the

Table 2. Results of the Kinetic and Equilibrium Analyses for the Cp*MoCl(PMe₃)₂/N₂ System

<i>T</i> , °C	10 ³ [Cp*MoCl(PMe ₃) ₂] ₀ , M	10 ³ [N ₂], M	<i>K</i> _{eq} , M ⁻¹	10 ³ <i>k</i> ₁ , M ⁻¹ s ⁻¹
8	7.77 ± 0.25	5.68 ± 0.04	950 ± 39	3.11 ± 0.14
16	2.52 ± 0.08	5.46 ± 0.03	357 ± 16	7.04 ± 0.31
20	3.58 ± 0.11	5.43 ± 0.03	154 ± 7	8.58 ± 0.39
25	2.21 ± 0.07	5.24 ± 0.03	100 ± 3	14.3 ± 0.4

**Figure 2.** Plot of $\ln(k_1/T)$ versus $1/T$ for the N₂ addition to Cp*MoCl(PMe₃)₂.**Figure 3.** Plot of $\ln(K_{\text{eq}})$ versus $1/T$ for equilibrium 3.

CO addition. Even on a pure qualitative basis, the CO addition occurs within a few minutes at low temperatures, whereas the N₂ addition takes place over a few hours at more elevated temperatures. A larger temperature range could not be investigated, because the reaction is exceedingly slow at lower temperatures and the variability of the atmospheric pressure introduces errors, whereas significant thermal decomposition of the 16-electron material prevents the achievement of a stable equilibrium at higher temperatures.

The activation parameters from the Eyring analysis (Figure 2) are $\Delta H^\ddagger = 14.0 \pm 1.0$ kcal/mol and $\Delta S^\ddagger = -20 \pm 3$ cal·mol⁻¹·K⁻¹ for the N₂ addition. It is notable that the activation enthalpy is three times as large as that of the CO addition. It is also to be noted that the value of the *K*_{eq} decreases with an increase in temperature, as expected. A plot of the $\ln K_{\text{eq}}$ versus $1/T$ (Figure 3) provides the thermodynamic parameters for this reaction, $\Delta H = -22.8 \pm 2.1$ kcal·mol⁻¹ and $\Delta S = -67 \pm 7$ cal·mol⁻¹·K⁻¹.

(19) Wilkins, R. G. *Kinetics and Mechanism of Reactions of Transition Metal Complexes*, 2nd ed.; VCH: New York, 1991; p 465.

Table 3. Geometrical Parameters for MP2 Geometry-Optimized 16-Electron CpMoCl(PH₃)₂ and the 18-Electron CpMoCl(PH₃)₂L (L = CO, N₂)

	exptl Cp*MoCl(dppe) ^a (S = 1)	calcd CpMoCl(PH ₃) ₂	
		(³ A'')	(¹ A')
Mo–Cp (av)/Å	2.335(4)	2.363	2.356
Mo–Cl/Å	2.415(1)	2.499	2.464
Mo–P/Å	2.421(1)	2.561	2.496
Cl–Mo–P/deg	83.59(4), 92.94(5)	88.96	93.41
P–Mo–P/deg	78.71(4)	94.56	83.77
E/hartrees		–290.6195	–290.6021

	exptl Cp*MoCl(PMe ₂ Ph) ₂ (CO) ^a (S = 0)	calcd		exptl CpMoCl(PH ₃) ₂ (N ₂) ^d (S = 0)
		CpMoCl(PH ₃) ₂ (CO) ^b (¹ A')	CpMoCl(PH ₃) ₂ (N ₂) ^c (¹ A')	
Mo–Cp (av)/Å	2.335(9)	2.385	2.363	2.328
Mo–Cl/Å	2.577(5)	2.594	2.585	2.527
Mo–P/Å	2.474(2)	2.508	2.513	2.464
Mo–L/Å	1.87(1)	1.888	1.917	2.158
Cl–Mo–P/deg	78.1(1)	75.53	77.59	77.33
P–Mo–P/deg	116.6(1)	132.82	125.51	114.4
Cl–Mo–L/deg	128.9(7)	120.08	130.60	131.50
P–Mo–L/deg	76.4(4)	81.64	80.39	76.97
E/hartrees		–403.6099	–399.7825	

^a See ref 11. ^b The energy of CO was calculated at –112.8948 hartrees. ^c The energy of N₂ was calculated at –109.1185 hartrees. ^d The bond lengths and angles are calculated from published fractional coordinates. No esd's are available. See ref 31.

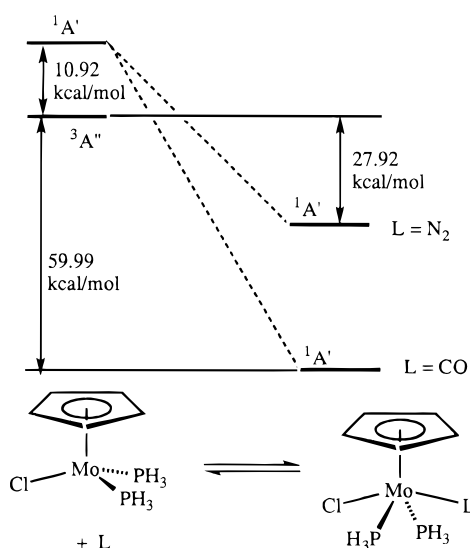
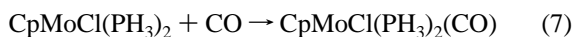


Figure 4. Total energies of the MP2 geometry-optimized CpMoCl(PH₃)₂ and CpMoCl(PH₃)₂L (L = CO, N₂) adducts. The right hand side energies are plotted as $E\{\text{CpMoCl(PH}_3)_2\text{L}\} - E\{\text{L}\}$.

Theoretical Calculations. (a) Fully Optimized Geometries.

In order to probe and compare the energetic factors regulating the addition reactions discussed above, theoretical investigations of two model systems (eqs 7 and 8) were performed. The Cp* and PMe₃ ligands of the real system are replaced with Cp and PH₃ ligands for reasons of computational economy. The calculations consisted of unrestricted open-shell SCF followed by second-order Møller–Plesset (MP2) geometry optimizations (see Experimental Section).



The optimized geometrical parameters are collected in Table 3 and the normalized energetic picture is summarized in Figure 4. For all of the species involved, the bond distances are in reasonably good agreement with experiment. The discrepancy

between the angular parameters in ³A'' CpMoCl(PH₃)₂ and the crystallographically characterized Cp*MoCl(dppe) is attributable to the geometrical constraints of the ethylene backbone in the dppe ligand. As for the 18-electron compounds CpMoCl(PH₃)₂L (L = CO or N₂), there is a discrepancy between the experimental and calculated P–Mo–P and Cl–Mo–L angles. In particular, the experimental P–Mo–P angles are much smaller than the optimized ones. This phenomenon may be attributed to the steric repulsion between the bulky Cp* and PMe₃ ligands. In addition, the rather large discrepancy in the Mo–N₂ distance may be caused by the inaccuracy of the experimental measurement, since the structure of Cp*MoCl(PMe₃)₂(N₂) shows N₂/Cl disorder.³¹

According to the calculations, the 16-electron system has a triplet ground state, as experimentally observed for the Ring-MoCl₂ system (Ring = Cp, L = PMe₂Ph; Ring = Cp*, L = PMe₃, PMe₂Ph or L₂ = dppe).^{10,11} The four highest energy electrons reside in three metal based orbitals which can be related to the t_{2g} set in octahedral complexes. These orbitals are directed away from the ligands and can be utilized for π-bonding. In fact, the π-interaction between the chlorine lone pairs and these orbitals probably helps stabilize energetically these unsaturated 16-electron Mo(II) complexes.¹⁰ The cost of pairing the electrons in this system (e.g. the triplet–singlet gap) is calculated as 10.92 kcal/mol. The calculations on the 18-electron CO and N₂ adducts indicate a bond energy of 38.8 kcal/mol for the Mo–N₂ bond and 70.9 kcal/mol for the Mo–CO bond with respect to ¹A' CpMoCl(PH₃)₂ or 27.9 and 60.0 kcal/mol, respectively, with respect to the ground state ³A'' CpMoCl(PH₃)₂. The bond formation stabilization along the spin singlet surface is indicated in Figure 4 by the dashed lines. These results are in qualitative agreement with the experimental observation of a quantitative CO addition and an equilibrium N₂ addition.

(b) Reaction Coordinates. Calculations have also been carried out at various points along the reaction coordinates related to the CO and N₂ addition processes by keeping fixed Mo–C or Mo–N bond lengths, respectively, and letting the program optimize all the other geometrical parameters. The

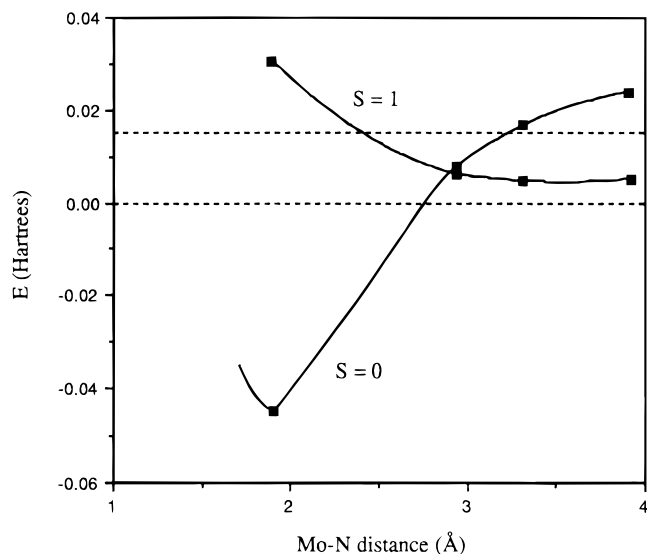


Figure 5. Calculated MP2 reaction coordinate for the addition of N_2 to $\text{Cp}^*\text{MoCl}(\text{PMe})_2$. The energy axis is normalized relative to the calculated total energy of the two reagents at infinite distance. The upper dashed line corresponds to the energy of $^1\text{A}' \text{CpMoCl}(\text{PH}_3)_2 + \text{N}_2$ at infinite distance.

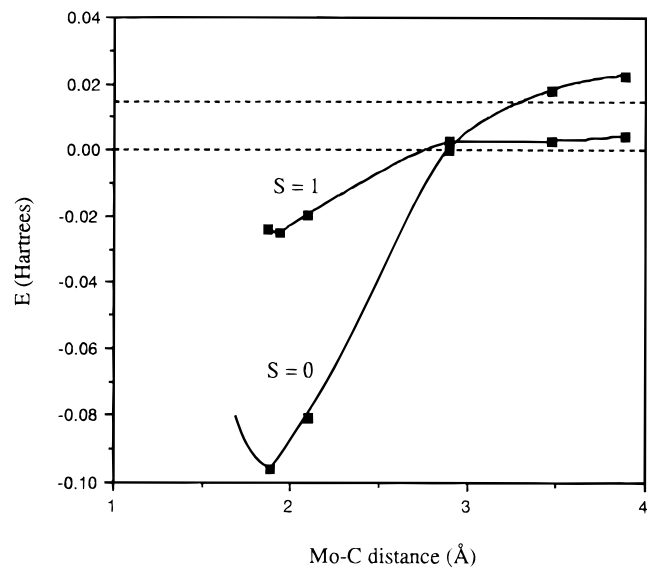


Figure 6. Calculated MP2 reaction coordinate for the addition of CO to $\text{Cp}^*\text{MoCl}(\text{PMe})_2$. The energy axis is normalized relative to the calculated total energy of the two reagents at infinite distance. The upper dashed line corresponds to the energy of $^1\text{A}' \text{CpMoCl}(\text{PH}_3)_2 + \text{CO}$ at infinite distance.

results and graphical interpolations are shown in Figure 5 for the N_2 addition and in Figure 6 for the CO addition.

As is clearly shown by Figure 5, the approach of N_2 continuously raises the energy of the triplet curve, while the singlet excited state of the 16-electron precursor is stabilized and leads to the bound dinitrogen complex. An initial increase in energy, however, is observed also for the singlet curve. This may be attributed to an initial $\text{PH}_3\text{-N}_2$ van der Waals repulsive interaction. In other words, the two phosphine ligands need to distort (by bending away from the incoming ligand) in order to allow the N_2 molecule to reach a suitable distance for a bonding interaction with the metal center to be established. This is most clearly shown by the sequence of partially optimized geometries in Figure 7. At the Mo-N distance of 3.917 Å, the distortion of the two PH_3 ligands away from the incoming N_2 ligand and toward the Cl ligand is already significant, while the N_2 ligand

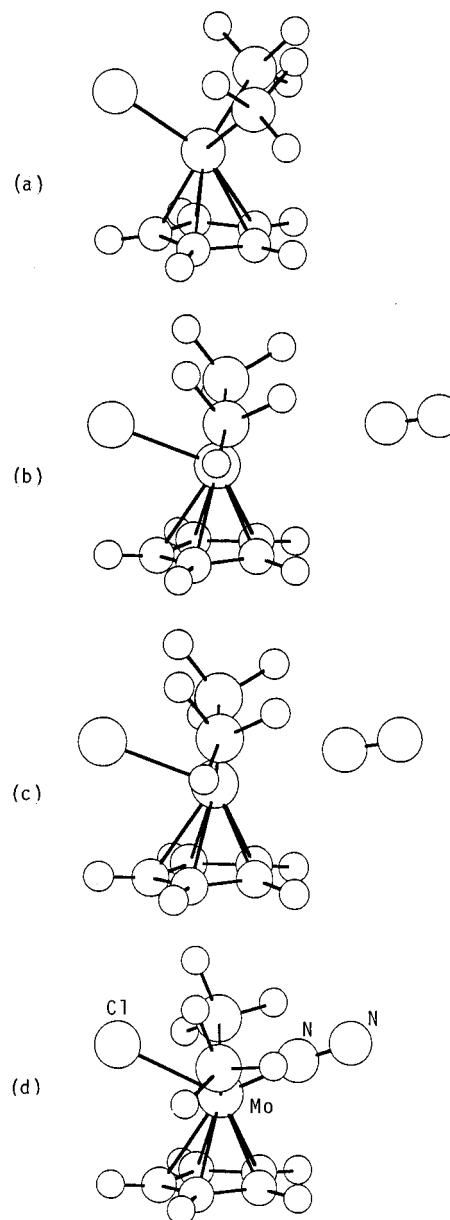


Figure 7. Four representative geometries along the N_2 addition coordinate to $^1\text{A}' \text{CpMoCl}(\text{PH}_3)_2$: (a) optimized $^1\text{A}' \text{CpMoCl}(\text{PH}_3)_2$ (N_2 at infinite distance); $\text{P-Mo-P} = 83.77^\circ$; (b) $\text{Mo}\cdots\text{N} = 3.917 \text{ \AA}$, $\text{P-Mo-P} = 107.50^\circ$; (c) $\text{Mo}\cdots\text{N} = 2.917 \text{ \AA}$, $\text{P-Mo-P} = 110.17^\circ$; (d) $\text{Mo}\cdots\text{N} = 1.917 \text{ \AA}$, $\text{P-Mo-P} = 125.51^\circ$.

has not yet established a significant stabilizing interaction. While the bending of the P-Mo-P plane away from the N_2 ligand is most dramatic at the early stages of the addition process, the P-Mo-P angle gradually opens from the value of the starting 16-electron complex (83.77°) to that of the final product (125.51°) along the reaction coordinates (see Figure 7). The spin crossover is calculated at a Mo-N distance of ca. 2.9 Å and at an energy of 4.2 kcal/mol relative to the two reagents at infinite distance. At the Mo-N distance corresponding to the energy minimum for the singlet state (1.917 Å), the triplet state shows lengthening of all Mo-ligand distances relative to those in the geometry optimized singlet molecule (0.097 Å for $\text{Mo-C}(\text{Cp, average})$, 0.182 Å for Mo-Cl , and 0.072 Å for Mo-P). The two PH_3 ligands are bent away from the CO ligand and toward the Cl ligand (see Figure 8a).

The trends observed for the N_2 addition coordinate are in part reproduced for the CO addition coordinate. The spin singlet surface is qualitatively similar, including the initial increase in

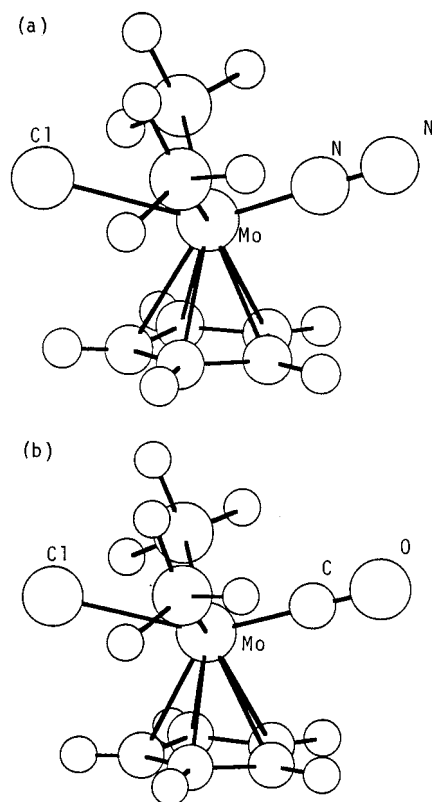


Figure 8. Partially optimized MP2 geometries (fixed Mo–L distances) for $^3A''$ CpMoCl(L)(PH₃)₂: (a) L = N₂, Mo–N = 1.917 Å; (b) L = CO, Mo–C = 1.888 Å.

energy attributed to the PH₃–CO van der Waals repulsive interaction. However, the singlet curve descends in energy more rapidly and crosses the zero energy level (relative to the two reagents at infinite distance) at 2.89 Å vs 2.77 Å for the corresponding N₂ curve. The spin triplet curve shows an initial energy increase upon approaching the CO ligand, analogous to the triplet curve of the N₂ addition coordinate (cf. Figures 5 and 6). However, the continued CO approach results in an energy decrease and leads to an energy minimum at Mo–C = 1.929 Å. The spin crossover point for the CO addition coordinate is calculated at ca. 2.9 Å for the Mo–C distance and at an energy of ca. 1.3 kcal/mol. This energy is lower than the highest point along the spin triplet curve (i.e. >2.6 kcal/mol). Although the spin triplet curve is repulsive for N₂ and attractive for CO, the molecular distortions are similar for the two ligand additions. The partially optimized $^3A''$ CpMoCl(PH₃)₂(CO) molecule at the Mo–C distance of 1.929 Å is shown in Figure 8b, which can be directly compared with the corresponding N₂ system in Figure 8a. The Mo–C(Cp, average), Mo–Cl, and Mo–P bonds are 0.126, 0.144, and 0.036 Å longer than those of the optimized singlet molecule.

Discussion

A first point of discussion concerns the energetic stabilization of the open-shell (Ring)MoClL₂ systems (Ring = Cp, Cp*; L = tertiary phosphine) by adopting an unpaired-spin configuration. It is common to find stable open-shell organometallics with more than one unpaired electron. While 16-electron highly reactive (presumably spin singlet) intermediates such as M(CO)₅ (M = Cr, Mo, W),²⁰ M(CO)₄ (M = Ru,⁵ Os²¹), CpM(CO)₃ (M

= V, Nb, Ta),²² and CpRh(CO)²³ efficiently bind donors as poor as rare gases, corresponding spin triplet intermediates, e.g. Fe(CO)₄,²⁴ and CpCo(CO),⁸ apparently do not. Since saturated (18-electron) organometallic complexes are forced into a spin singlet configuration by large HOMO–LUMO gaps, the binding of a ligand to a spin triplet 16-electron complex is a trade-off between the cost of pairing the electrons and the energetic gain of the metal–ligand bond along the spin singlet surface. In 1974, Calderazzo recognized that the unusually low bond dissociation enthalpy of 13.1(10) kcal/mol for the V–CO bond in Cp₂VI(CO) could be related to the change of spin state, since Cp₂VI has two unpaired electrons. A similar conclusion was proposed by Brintzinger in 1975 for the Cr–CO bond in Cp₂Cr(CO) ($\Delta H = 18.8(5)$ kcal/mol).²⁵ A change of spin state could also be contributing to the low BDE for Co–CO (12.9(2) kcal/mol) in TpCo(CO)₂ (Tp = hydrotris(3-isopropyl-5-methylpyrazolyl)borate).⁴

Given the repulsive Mo–N₂ interaction along the triplet curve (Figure 5) and the generally stronger binding of N₂ relative to rare gases and hydrocarbons, the experimental observation of a Curie $S = 1$ system for solutions of Cp*MoCl(PMe₃)₂ in *n*-heptane under Ar in the temperature range 198 to 291 K (Evans' method)¹⁰ strongly suggests that this 16-electron compound does not establish any interaction with rare gases or with hydrocarbons. Neither is an interaction established with THF. This is shown by the invariance of the contact-shifted NMR spectrum of Cp*MoClL₂ (L = PMe₃, PMe₂Ph or L₂ = dppe) to the addition of free THF in C₆D₆.¹¹ However, Cp*MoCl(PMe₃)₂ is able to form bonds with dinitrogen and carbon monoxide. For the model CpMoCl(PH₃)₂ system, our MP2 calculations (Figure 4) indicate that the strengths of the Mo–N₂ and Mo–CO bonds are sufficient to more than compensate for the cost of pairing the electrons. The validity of the MP2 calculation, at least at a qualitative level, is indicated by the following points: (a) the triplet state for the 16-electron CpMoCl(PH₃)₂ is 10.92 kcal/mol lower in energy than the singlet state, in agreement with the experimentally determined $S = 1$ state for Cp*MoCl(PMe₃)₂ and Cp*MoCl(dppe);^{10,11} (b) the greater binding energy for CO versus N₂ is in agreement with the quantitative CO addition and with the equilibrium addition of N₂; and (c) the calculated energy difference between the $^3A''$ 16-electron complex and the $^1A'$ 18-electron N₂ complex is –27.92 kcal/mol, i.e. in reasonable agreement with the experimentally determined value (–22 ± 2 kcal/mol). In fact, given that the MP2 method tends to overestimate the electronic correlation and given that the spin singlet system is more correlated than the spin triplet system, it was anticipated that the calculated BDE should exceed the experimental value. For the same reason, the calculated triplet–singlet gap is likely an underestimation of the true gap. A similar theoretical analysis of the reaction between the 15-electron CpMCl₂(PH₃) and PH₃ to give the 17-electron CpMCl₂(PH₃)₂ (M = Cr, Mo) has indicated that the quartet–doublet gap in the 15-electron systems is larger than the M–PH₃ bond energy for M = Cr but smaller for M = Mo.²⁶

Coming now to the kinetic issue and in particular to the effect of the spin state change on the activation barrier, following the

(22) George, M. W.; Haward, M. T.; Hamley, P. A.; Hughes, C.; Johnson, F. P. A.; Popov, V. K.; Poliakoff, M. *J. Am. Chem. Soc.* **1993**, *115*, 2286–2299.

(23) Rest, A. J.; Whitwell, I.; Graham, W. A. G.; Hoyano, J. K.; McMaster, A. D. *J. Chem. Soc., Dalton Trans.* **1987**, 1181–1190.

(24) Poliakoff, M.; Weitz, E. *Acc. Chem. Res.* **1987**, *20*, 408–414.

(25) Wong, K. L. T.; Brintzinger, H. H. *J. Am. Chem. Soc.* **1975**, *97*, 5143–5146.

(26) Cacelli, I.; Keogh, D. W.; Poli, R.; Rizzo, A. *New J. Chem.* **1997**, *21*, 133–135.

(20) Wells, J. R.; Weitz, E. *J. Am. Chem. Soc.* **1992**, *114*, 2783–2787.

(21) Bogdan, P. L.; Weitz, E. *J. Am. Chem. Soc.* **1990**, *112*, 639–644.

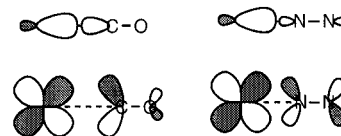
Table 4. Comparative Rates of CO and N₂ Additions to 16-Electron Organometallic Complexes

complex	S	solv/T (°C)	$k_1/M^{-1} s^{-1}$ (CO add.)	$k_2/M^{-1} s^{-1}$ (N ₂ add.)	ref
CpV(CO) ₃	0?	heptane/25	1.3×10^8	1.5×10^8	22
CpNb(CO) ₃	0?	heptane/25	7.6×10^6	4.9×10^6	22
CpTa(CO) ₃	0?	heptane/25	5.0×10^6	2.9×10^6	22
CpW(CH ₃)(CO) ₂	0?	heptane/rt ^a	$2.0(2) \times 10^7$	$4.7(5) \times 10^6$	30
Cp*MoCl(PMe ₃) ₂	1	THF/25	$2.2(2) \times 10^1$	$1.47(7) \times 10^{-2}$	b

^a rt = room temperature. ^b This work.

general treatment of radiationless nonadiabatic transitions,²⁷ the rate of a reaction involving a spin state change is affected by two parameters: a classical activation enthalpy (i.e. the enthalpy necessary for bringing the geometry of the activated complex to a configuration where the two spin states have an identical geometry and similar energy) and the so-called prohibition factor which determines the probability of intersystem crossing. The latter can be treated as a purely entropic factor in the rate law. Spin-orbit interactions are the main cause for the breakdown of the selection rule that forbids intersystem crossing and are responsible for high transmission probabilities, especially for the 4d and 5d metals. This factor has been invoked to discount a "spin block" to organometallic reactions.⁴ Nevertheless, a spin state change may still slow a reaction for mere enthalpic reasons.

The comparison between the activation barriers for the CO and N₂ additions illuminates this case. The k_1 values extrapolated to room temperature for the addition of CO ($22 \pm 2 M^{-1} s^{-1}$) and N₂ ($0.0147 \pm 0.0007 M^{-1} s^{-1}$) differ by over 3 orders of magnitude. There is no other example, to the best of our knowledge, of a comparative kinetic study of the addition of the isosteric and isolobal CO and N₂ to spin triplet 16-electron complexes or to any other complex where such addition would cause a spin state change. None of the systems mentioned in the Introduction for which the CO addition kinetics have been measured seem to form stable adducts with N₂. The spin triplet [CpFe(dippe)]⁺ (dippe = bis(1,2-diisopropylphosphino)ethane) complex is capable of adding both CO and N₂ (the first quantitatively and the second in an equilibrium process), but no rate data were provided for either reaction.²⁸ It was only shown by ¹H-NMR that the 16-electron [CpFe(dippe)]⁺ complex and its 18-electron N₂ adduct are in the slow exchange regime at room temperature under N₂. There are, however, kinetic studies of the CO and N₂ additions to high-energy photolytic intermediates. In all those cases (see Table 4) it is unclear whether genuine 16-electron species or solvent adducts are involved and whether their ground state is indeed a singlet. IR studies in low-temperature matrices indicated that the CpM-(CO)₃ complexes (M = V, Nb, Ta) have a C_s symmetry pointing to a solvent adduct or to a spin singlet 16-electron species (C_{3v} symmetry would be expected for a S = 1 ground state). The largest difference in second-order rate constants for these systems (Table 4) is approximately a factor of 4 in favor of the CO addition. This small difference may be explained by Hammond's postulate,²⁹ since the CO adduct is thermodynamically more stable than the N₂ adduct. It is clear, therefore, that there is no reason to expect such a dramatic difference in rates for the CO and N₂ addition to an unsaturated compound such

Scheme 1

as Cp*MoCl(PMe₃)₂, were it not for the necessity to reach a suitable geometry to allow the spin state change.

The MP2 calculations along the ligand addition coordinate have shed further light onto the matter. A first reason to expect a lower barrier for the CO vs the N₂ addition is the difference in orbital diffuseness between the two incoming ligands (Scheme 1). CO and N₂ interact with transition metals in a qualitatively identical manner: the HOMO engages in a σ bonding interaction with an empty metal-based orbital, and the LUMO establishes a π (back) bonding interaction with a filled metal orbital. This interaction is energetically stabilizing only for the spin singlet CpMoCl(PH₃)₂ moiety, whereas it will be repulsive for the corresponding spin triplet state. Both the donor HOMO and the acceptor LUMO are more diffuse for CO than for N₂ and the orbital energies are also more suitably placed for the CO vs the N₂ (the HOMO has higher energy for CO, i.e. CO is a better nucleophile, and the LUMO has lower energy for CO, i.e. CO is a better electrophile). It is thus apparent that the CO ligand will be able to interact with the metal and sufficiently stabilize the spin singlet system at a longer M-L distance relative to N₂. This is indeed verified by the calculations, the energy of the spin singlet curve descending earlier for CO vs N₂ along the L addition coordinate, cf. Figure 5 and 6. A second and more important difference, however, is evident from the calculation. The N₂ ligand establishes a weaker bond with the Mo center relative to all the other ligands already present in the coordination sphere. Thus, the approach of N₂ to the Mo center along the spin triplet surface is repulsive and the transition state corresponds to the crossover point between the two spin surfaces. On the other hand, after the initial interligand van der Waals repulsive interaction, the triplet CO curve is attractive until beyond the crossover point with the singlet curve and leads to a bound state. The barrier in this case is due to the initial deformation of the ³A'' CpMoCl(PH₃)₂ coordination sphere upon approach of CO and can be attributed to the CO...PH₃ van der Waals repulsion, with little contribution, if any, from the Mo-CO bond formation.

The calculations do not quantitatively reproduce the measured activation barriers. The calculated highest energy along the CO addition coordinate is ca. 2.6 kcal/mol, while the experimental activation enthalpy is 5.0 ± 0.3 kcal/mol (corresponding to a ΔE^* of ca. 5.5 kcal/mol). The larger experimental value is to be attributed to the greater van der Waals repulsive interaction of the CO ligand with the Cp* and PMe₃ ligands relative to the Cp and PH₃ ligands used in the model system. The discrepancy between the experimental activation barrier for the N₂ addition ($\Delta H^* = 14.0 \pm 1.0$ kcal/mol or ΔE^* ca. 14.5 kcal/mol) and the calculated highest energy of 4.2 kcal/mol at the spin crossover point can only be attributed to the inadequacy of the computational method. The calculation of a repulsive triplet curve for the N₂ addition, however, indicates very strongly that the discrepancy between the rates of addition of CO and N₂, especially when compared with those to other 16-electron complexes (Table 4) can only be attributed to the necessity to reach a high energy spin crossover point.

(27) Turro, N. J. *Modern Molecular Photochemistry*; Benjamin/Cummings Publishing Co.: Menlo Park, CA, 1978.

(28) de la Jara Leal, A.; Tenorio, M. J.; Puerta, M. C.; Valerga, P. *Organometallics* **1995**, *14*, 3839-3847.

(29) Hammond, G. S. *J. Am. Chem. Soc.* **1955**, *77*, 334-338.

(30) Virrels, I. G.; George, M. W.; Johnson, F. P. A.; Turner, J. J.; Westwell, J. R. *Organometallics* **1995**, *14*, 5203-5208.

(31) Baker, R. T.; Morton, J. R.; Preston, K. F.; Williams, A. J.; Le Page, Y. *Inorg. Chem.* **1991**, *30*, 113-116.

It should be mentioned here that Brintzinger *et al.* rationalized the fast addition of CO to spin triplet molybdenocene by carrying out theoretical calculations along the CO addition coordinate and showed that the spin surface crossing occurs at a relatively low activation energy.¹ In the case investigated by Brintzinger, a lower level of theory (EHMO) was used and the Mo–Cp distance was kept fixed along the reaction coordinate. Therefore, the calculated spin triplet curve was repulsive in that case. However, the stabilization of the spin singlet curve occurs at a relatively long Mo–C distance where the spin triplet curve is not yet sufficiently repulsive, resulting in a low activation barrier in agreement with the experiment.¹

Conclusions

A comparison of the addition rates of the isosteric and isolobal CO and N₂ ligands to a spin triplet 16-electron organometallic molecule has been carried out for the first time. The large

difference in the addition rates to Cp*MoCl(PMe₃)₂ points to the importance of the molecular rearrangements that are necessary to reach the spin crossover point for determining the height of the activation barrier. While the N₂ addition raises significantly the energy of the spin triplet surface before the spin singlet becomes sufficiently stabilized, the CO addition results in an attractive interaction all the way after the initial van der Waals activation barrier. While spin change selection rules as a factor in slowing down organometallic reaction should probably be neglected in some cases,⁴ the concept that a spin state change can slow down organometallic reactions is quite appropriate for some systems for mere enthalpic reasons.

Acknowledgment. We are grateful to the National Science Foundation (Grant No. CHE-9508521) for support.

JA960786U